Temporal Variability of Zooplankton from ADCP Backscatter Time Series Data at the Central Irminger Sea (CIS) Site

-B. Sc. Physics of the Earth System-

Meteorology, Oceanography, Geophysics

Mathematisch-Naturwissenschaftliche Fakultät

Christian-Albrechts-Universität zu Kiel

Maren Elisabeth Richter

Matriculation Number: 1005653

June 23, 2014

First Examiner: Dr. rer. nat. Johannes Karstensen

Second Examiner: Dr. rer. nat. Helena Hauss

Abstract

Diel vertical migration (DVM) of zooplankton at the Central Irminger Sea (CIS) Site ($59.7° N - 39.7° E$) was studied using targetstrength calculated from ADCP echo intensity. Daily and seasonal patterns were interpreted using hydrographical data and vertical velocities of the scatterers from ADCP measurements were examined. Data obtained between summer 2004 and summer 2007 as well as during summer 2011 and summer 2012 was used. The data shows that the zooplankton at the CIS site perform normal vertical migration with ascent starting at dusk and descent one hour before dawn. Vertical velocities were between 1 and 4 cm/s with velocities being higher during the descent than during ascent. Two distinct deep scattering layers were visible throughout the time of the deployments one around 400m and one around 600m depth. There was some evidence of seasonal changes in DVM. In particular, the depth of the mixed layer had an influence on the strength of the backscatter signal and the vertical extent of the migration.

Zusammenfassung

Vertikale Migration von Zooplankton in der Zentalen Irmingersee (CIS) bei $59.7°N$ und $-39.7°E$ wurde mithilfe von Rückstreustärke aus ADCP Daten untersucht. Tägliche und saisonale Variationen wurden mithilfe hydrographischer Daten interpretiert und die vertikale Geschwindigkeit der Rückstreuer aus ADCP Daten betrachtet. Die verwendeten Daten wurden zwischen Sommer 2004 und Sommer 2007 sowie Sommer 2011 und Sommer 2012 gesammelt. Die Daten zeigen, dass das Zooplankton an der CIS Verankerung normale vertikale Migration vollführt. Der Aufstieg beginnt bei Sonnenuntergang und der Abstieg ca. eine Stunde vor Sonnenaufgang. Zwei tiefe Rückstreuhorizonte um 400 und 600m Tiefe sind während des gesammten Untersuchungszeitraums deutlich zu erkennen. Es gab Anzeichen für saisonale Änderungen der vertikalen Migration. Insbesondere ist die Stärke der Rückstreuung korreliert mit der Tiefe der durchmischten Deckschicht, die auch einen Einfluss auf die vertikale Ausdehnung der Migration zu haben scheint.

Contents

1 Introduction

In the wake of global warming, interest in vertical migration of zooplankton has increased as this is suspected to be a pathway for removing organic carbon from the surface layer and therefore from contact with the atmosphere. Changes in migration behaviour or in migrant biomass may therefor be linked to ocean CO_2 uptake (*Longhurst et al.*, 1990). As the Irminger Gyre is also thought to be a region in which Labrador Sea Water can be formed, carbon entrained into the deeper layers would be removed from exchange with the atmosphere for a long period of time (*Våge et al.*, 2011). Vertically migrating zooplankton also plays a role in macronutrient (nitrogen, phosphorous) exchange across the thermocline (*Longhurst et al.*, 1989). The zooplankton ingest particulate organic compounds in the photic zone through grazing on phytoplankton, protozoans and detritus and continue excreting particulate and dissolved organic and inorganic compounds at depth. They thereby form a pathway for transporting nitrogen and other nutrients across the pycnocline (*Longhurst and Harrison*, 1988; *Longhurst et al.*, 1989).

There are three main patterns of diel vertical migration (DVM). The most common, also referred to as 'nocturnal migration', is the nighttime ascent where zooplankton ascend in the evening to spend the night in the food-rich upper layers and descend at dawn to the dark deeper layers. Less common is a slow descent after the initial dusk ascent and a subsequent ascent before the dawn descent. This behaviour is known as the 'midnight-sink' or 'twilight-migration'. The third pattern is reverse migration with ascent at dawn and descent at dusk. Different theories have been proposed as to why zooplankton migrate and different proximate and ultimate reasons discussed. These theories have been grouped into three categories depending on their proposed ultimate reasons: Vertical migration due to a gain of metabolic or demographic advantage, vertical migration to avoid light-related mortality and vertical migration in order to optimize the exploitation of food-sources. The most accepted of these is the predation-avoidance hypothesis though other factors may be involved (*Lampert*, 1989). Larger and more strongly pigmented species are more susceptible to visually hunting predators and therefore exhibit a more pronounced DVM with body morphology also playing a role for larger taxa (*Hays* *et al.*, 1994). This in turn influences the behaviour of species from higher trophic levels who may in turn also exhibit DVM to follow their prey (*Hays*, 2003).

ADCPs are valuable for studying zooplankton concentration and migration in a qualitative way, as they are non-invasive, provide high temporal and spatial (in particular vertical) resolution and enable data collection year round. The latter point is especially important in high latitudes, as shipborne measurements are often impossible due to adverse weather conditions. Unlike ships ADCPs do not effect the vertical migration through shadowing or artificial light and the data is not biased by vessel displacement on repeat transects (*Benoit-Bird et al.*, 2009). Additionally, the high costs associated with research cruises would prevent long and continuous timeseries. ADCPs have been used in the study of zooplankton and zooplankton migration since the late 1980s (*Fischer and Visbeck*, 1993) and have contributed greatly to our understanding of the long term temporal variability of zooplankton distribution.

In a coupled physical-biological model study of the Irminger Sea for the year 2002, phyto- and zooplankton concentration relative to physical parameters were computed for four zones in the Irminger Sea (*Waniek and Holliday*, 2006). The model output was then compared with field data. In the CIS zone simulated phytoplankton bloom started at the beginning of May and continued for 70 days (when it collapsed due to insufficient light in the water column). Zooplankton populations were computed to increase with a 60 day delay compared to phytoplankton. Copepods are the most dominant species of zooplankton in the Irminger sea with the five most abundant copepod taxa being *C. finmarchicus, Pareuchaeta norvegica, C. Hyperboreus, Oithona* spp. and *Oncaea* spp.. These copepods are found in deep layers with some exhibiting seasonal migration (*Gislason*, 2003). The deep scattering layers also contain a wide variety of larger species, for an overview of fish species found in these layers see *Magnússon* (1996).

In this thesis, I will evaluate hydrographical and ADCP data to look for seasonal patterns in vertical zooplankton migration. I thereby assume that there is zooplankton which performs diel vertical migration at the study site and that the vertical extent of this migration is influenced by mixed layer depth.

2 Data and Methods

2.1 The Moorings

The Central Irminger Sea (CIS) site at $59.7°N - 39.7°E$ was part of the ANIMATE (Atlantic Network of Interdisciplinary Moorings and Time series for Europe) program and the EuroSITES European Ocean Observatory Network and is now part of the FP7 NACLIM (North Atlantic CLIMate) project. Each mooring contained one to two ADCPs and an array of MicroCATs. In this paper we will look at data from the CIS04 through CIS06 and CIS11 deployments, combined to cover the time from September 2004 through August 2007 and August 2011 to May 2012.

2.1.1 Hydrographical Data

The moorings were equipped with multiple MicroCATs deployed between 10m and 1000-1600m depth (see table 2 for an example). The MicroCats were of the type SBE-37 some of which could send data to shore via a telemetry satellite link every four hours. Temperature and salinity were recorded by all MicroCATs with some also recording pressure. For the final data set only the delayed mode data was used unless the instrument had been lost in which case telemetrically transferred data sets were used. Whenever possible MicroCAT data was calibrated using CTD casts.

Mixed layer depth is defined following *de Boyer Montégut et al.* (2004) as the depth at which the temperature difference to the surface exceeds or is equal to $-0.2\ °C$. Although the reason to undergo vertical migration is suspected to be escape from visually hunting predators, previous studies have found a higher correlation with solar and lunar phase than with actual surface illumination or relative rate of change of solar radiation (*Heywood*, 1996; *Benoit-Bird et al.*, 2009). It is suspected, that light intensity is used as cue to set the internal clock of the migrators. Because of this I did not look at actual surface illumination but concentrated on time of sunrise and sunset calculated using the air-sea toolbox. Conversion from pressure to depth was done using the Gibbs SeaWater (GSW) Oceanographic Toolbox of TEOS-10.

Table 1: Information on Moorings

Name	Time	Lat/Lon
cis04_up	19.9.2004-16.9.2005	59.6677 / -39.6929
cis04_do	18.9.2004-25.12.2004	59.6677 / -39.6929
cis05_up	19.9.2005-24.8.2006	59.6668 / -39.6990
cis05_do	18.9.2005-28.3.2006	59.6668 / -39.6990
cis06_up	24.8.2006-10.7.2007	59.6690 / -39.7078
cis06_do	29.8.2006-8.7.2007	59.6690 / -39.7078
cis11_up	13.8.2011-30.5.2012	59.6863 / -39.7300

2.1.2 Backscatter Data

The moorings contained two RDI Broadband ADCPs, one in up- the other in downward looking mode and were deployed for one year periods (Table 1). The ADCPs provided echo intensity data for the upper 800-1000m of the water column. Both the upward looking Workhorse Sentinel ADCPs and the downward looking Workhorse Long Ranger ADCPs were deployed at a nominal depth of 150m. Beam angle was 20° and beam configuration convex. Depth cell sizes were 16m for the downward looking ADCPs with the exception of the cis06 deployment where cell size was 8m, and 8m for the upward looking ADCPs. The upward looking ADCPs sampled with a frequency of 300Hz and the downward looking ADCPs at 75Hz. Between 10 and 70 profiles were made per time step (30 or 60 minutes) and ensemble averaged. For detailed configuration information see table 3. The cis11 deployment did not include a downward looking ADCP.

The ADCPs do some of the data processing internally, including conversion from beam coordinates to earth coordinates considering heading, pitch and roll of the instrument. Additionally, corrections for misalignment through local magnetic declination, an es-

Table 2: Table reproduced from *Fan et al.* (2013). CIS Mooring configuration and instrumentation example taken from the CIS third deployment (2004). Note that not every MicroCAT has a pressure sensor, and pressures are interpolated for measurements that do not have their own pressure sensor. The second MicroCAT is part of a slack surface telemetry unit which does not have tension pulling the wire vertical. Here, the measurements S, T, and P are salinity, temperature, and pressure, respectively. In addition, horizontal velocity measurements are denoted by U and V, and vertical velocity by W.

Nominal depth	Instrument	Measurement
10 m	SBE MicroCAT IM	S, T
10-30 m	SBE MicroCAT IMP	S, T, P
70 m	SBE MicroCAT IM	S, T
109 m	SBE MicroCAT IM	S, T
150 m	Teledyne-RDI Workhorse (upward)	U, V, W velocities 0-150 m, P
153 m	Teledyne-RDI Longranger ADCP (downward)	150-720 m, P
155 m	SBE MicroCAT IM	S, T
197 m	SBE MicroCAT IM	S, T
267 m	SBE MicroCAT IMP	S, T, P
372 m	SBE MicroCAT IM	S, T
548 m	SBE MicroCAT IMP	S, T, P
748 m	SBE MicroCAT IM	S, T
998 m	SBE MicroCAT IMP	S, T, P
1004 m	Aanderaa RCM-8 AVTP	T, P and U, V point velocities
1245 m	SBE MicroCAT IMP	S, T, P
1496 m	SBE MicroCAT IM	S, T
2283 m	McLean Sediment Trap	Sediment accumulation
2327 m	Aanderaa RCM-8 AVT	T and U, V point velocities

Table 3: Information on ADCP settings

Name	depth cell size (m)	sampling rate (min)	sample mode	pings per ensemble
cis04_up	8	60	1	70
cis04_do	16	30	1	10
cis05_up	8	60	1	70
cis05_do	16	30	1	10
cis06_up	8	60	1	70
cis06_do	8	30	1	20
cis11_up	8	60	1	70

timate of instrument depth and interpolation to a common time axis were performed (*Karstensen*, 2005). We then solve for the backscatter coefficient following the method given in *Deines* (1999) by means of the following equation:

$$\begin{aligned} S_v &= C10log_{10}\left(\left(T_x + 273.16\right)R^2\right) - L_{DBM} \\ &\quad - P_{DBW} + 2\alpha R + K_c\left(E - E_r\right) \end{aligned} \tag{1}$$

where S_v is the backscatter coefficient in decibels, C a parameter provided for the instrument, T_x the temperature of the transducer in degrees Centigrade, R the range along the beam to the scatterers (m), α the sound absorption coefficient of water (dB/m), θ the beam angle, L_{DBM} is $10log_{10}L$ (transmit pulse length L, meters), P_{DBW} is $10log_{10}P$ (transmit power P, Watts), K_c the factor of response to echo level of the receiver provided by the manufacturer, E echo intensity in counts and E_r reference level for E. R and the factor $2\alpha R$ were calculated following *Deines* (1999). The so derived backscatter gives us variations in target strength but no absolute values. Backscatter is caused by particles, plankton, small bubbles, sediment etc., in the watercolumn. Because the measurements were taken in an open ocean environment and bubbles only play a role in the upper few meters it is reasonable to attribute the observed backscatter principally to plankton and nekton. The received echo intensity is correlated with total zooplankton volume, dry weight and cross-sectional area (see for example *Flagg and Smith* (1989); *Jiang et al.* (2007)) but correlation may also be frequency specific (*Benoit-Bird*, 2009). ADCPs operated at typical frequencies are sensible to scatterers of sizes in the order of one millimeter and larger (*RDInstruments*, 1996). Apart from echo intensity, the ADCPs also recorded velocity profiles and temperature, salinity and pressure allowing to correct for vertical displacement of the moorings.

3 Results

3.1 Hydrographic Condition at the CIS Site

All CIS deployments lie within the Irminger Gyre. There was a mean stratification with fresher water at the surface and at depth and a salinity maximum between 200 and 400m depth. This was also observed by *Våge et al.* (2011). In general, the maximum salinity values which were found in the deep salinity maximum show very little to no interannual variability. The salinity minima found during summer are lower by roughly 0.5 compared to the maxima. The potential temperature minima in the deep were about 6 $°C$ lower than the summertime surface maxima. The maximum potential density anomaly (referred to as potential density from here onwards) showed almost no interannual variability with values around 27.76 ± 0.01 kg/m^3. During the cis04 deployment salinity ranged between 35.06 and 34.73, potential temperature between 3.28 $°C$ and 9.64 $°C$ and potential density between 26.96 kg/m^3 and 27.76 kg/m^3. Mixed layer deepening set in at the end of January and reached its maximum during February/March. Compared with the cis06 and cis11 deployments, the potential density gradient at the end of winter was steeper during the cis04 and cis05 deployments. In the time span of the cis05 deployment the salinity varied between 35.08 and 34.55, the potential temperature between 3.37 $°C$ and 9.18 $°C$ and the potential density between 26.92 kg/m^3 and 27.76 kg/m^3. Mixed layer shoaling started in April and deepening in December/January (Figure 1). The salinity during the cis06 deployment ranged between 35.08 and 34.65, the potential temperature between 3.43 $°C$ and 10.26 $°C$ and the potential density between 26.75 kg/m^3 and 27.75 kg/m^3. The mixed layer deepening set in earlier than during cis04 and cis05 starting in late November, shoaling started in late April. During the cis11 deployment salinity ranged between 35.04 and 34.66. Potential temperature varied between 9.92 $°C$ and 3.56 $°C$. Mixed layer shoaling began in April with a marked decrease in salinity at the surface. Gradual deepening of the mixed layer set in in late October and reached its maximum extent during March when potential density was virtually constant in the upper 1000m.

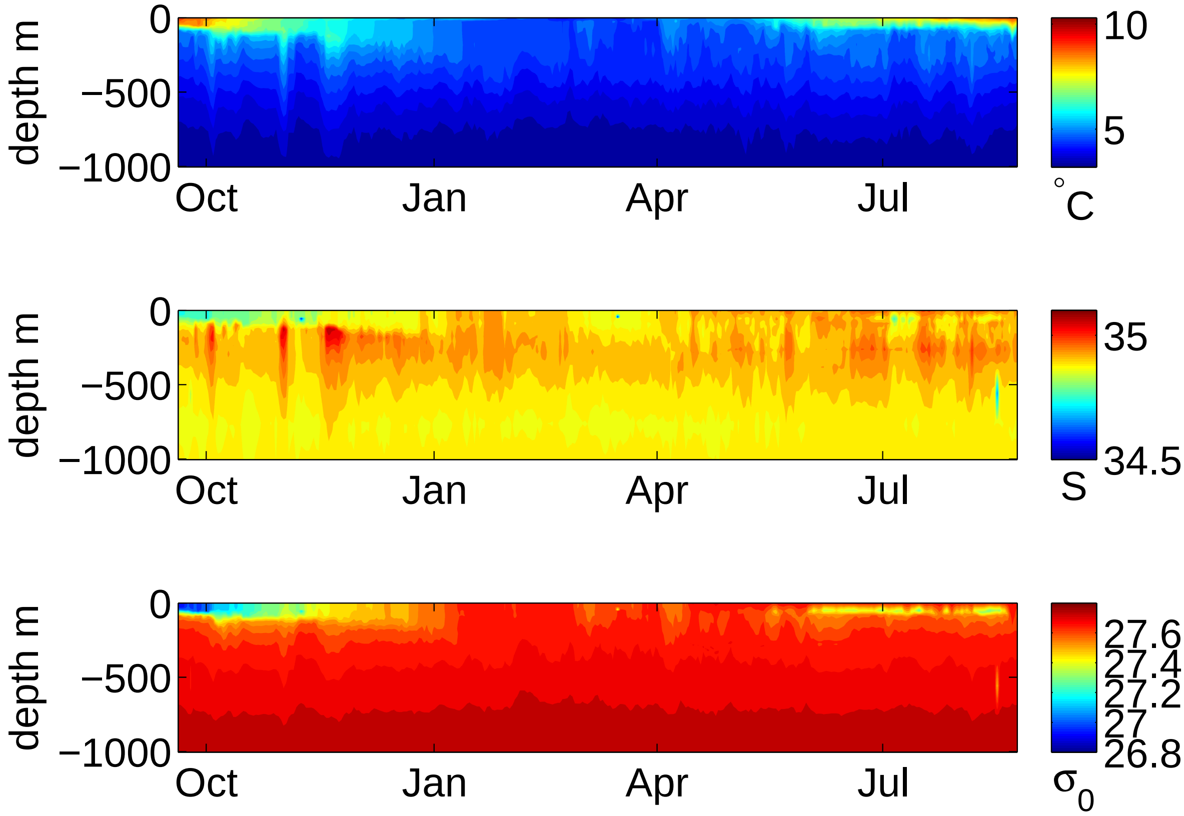

Figure 1: Hydrography from the cis05 deployment (summer 2005 to summer 2006). Upper panel shows potential temperature, middle panel salinity and bottom panel potential density anomaly referenced to the sea surface

3.2 Diel Cycles

3.2.1 Targetstrength in relation to the suncycle

In figure 2 the mean targetstrength in the upper 150m is shown with respect to the daytime. The black lines show the time of sunrise and sunset. During nighttime the targetstrength was lower than during daytime with the exception of the time between April and September during the cis06 and cis11 deployments. The decrease of targetstrength started roughly one hour before sunrise and continued to between sunset and one hour after sunset. The lowest mean targetstrengths were recorded during daytime between December and March.

3.2.2 Vertical velocity in relation to the suncycle

The vertical velocity of the migrating zooplankton was $1 - 2cm/s$ during ascent and $2 - 4cm/s$ during descent, with ascent and descent taking place roughly one hour after sunset and one hour before sunrise, respectively (Figure 3). Outside of these corridors the vertical velocity signal was very noisy, with no pattern visible.

3.2.3 Seasonal variation of daily cycle

To examine the seasonal variation of the daily cycle I looked at four specific points in the solar cycle. The solstices (summer and winter) are interesting because they mark the longest day and night respectively giving the zooplankton, provided it performs normal vertical migration, the least (summer solstice) and most (winter solstice) time to be in the surface layer. The two equinoxes (spring and autumn) then mark the time when day and night are equally long. In figures 4 to 6 two deep scattering layers can be identified at roughly 400 and 600m. These seven day means of targetstrength show the different daily cycles at specific points of the solar cycle. Around the spring equinox (panels a)) three echo maxima are visible, something that was not observed during the other seasons. The shape of the displacement in panels a) and c) (the equinoxes) is otherwise very similar. During noon the upper 300 to 400m were depleted of scatterers, these did

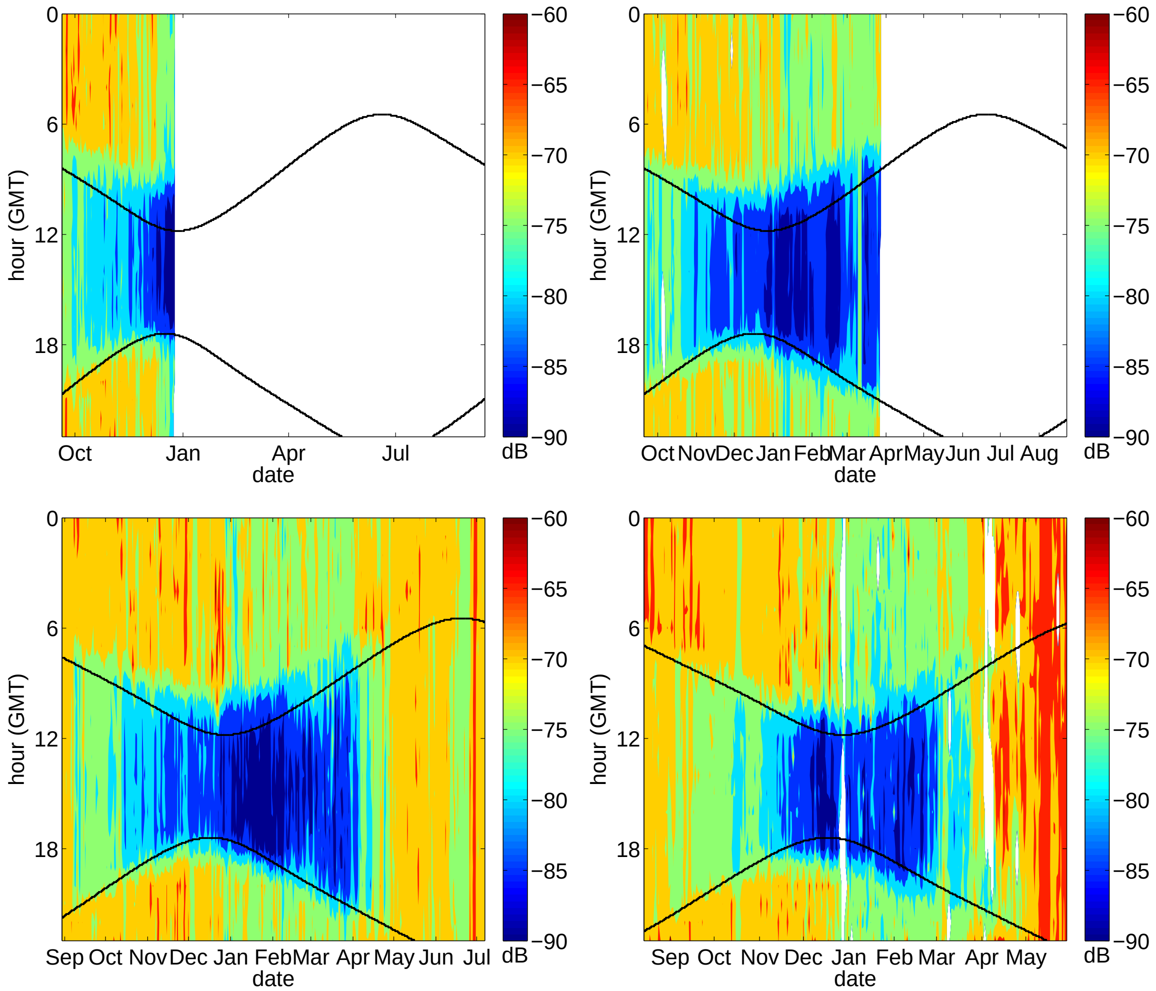

Figure 2: Mean targetstrength in the upper 150m, black lines show time of sunrise and sunset. From left to right and top to bottom: cis04 (summer 2004 to summer 2005), cis05 (summer 2005 to summer 2006), cis06 (summer 2006 to summer 2007), cis11 (summer 2011 to summer 2012).

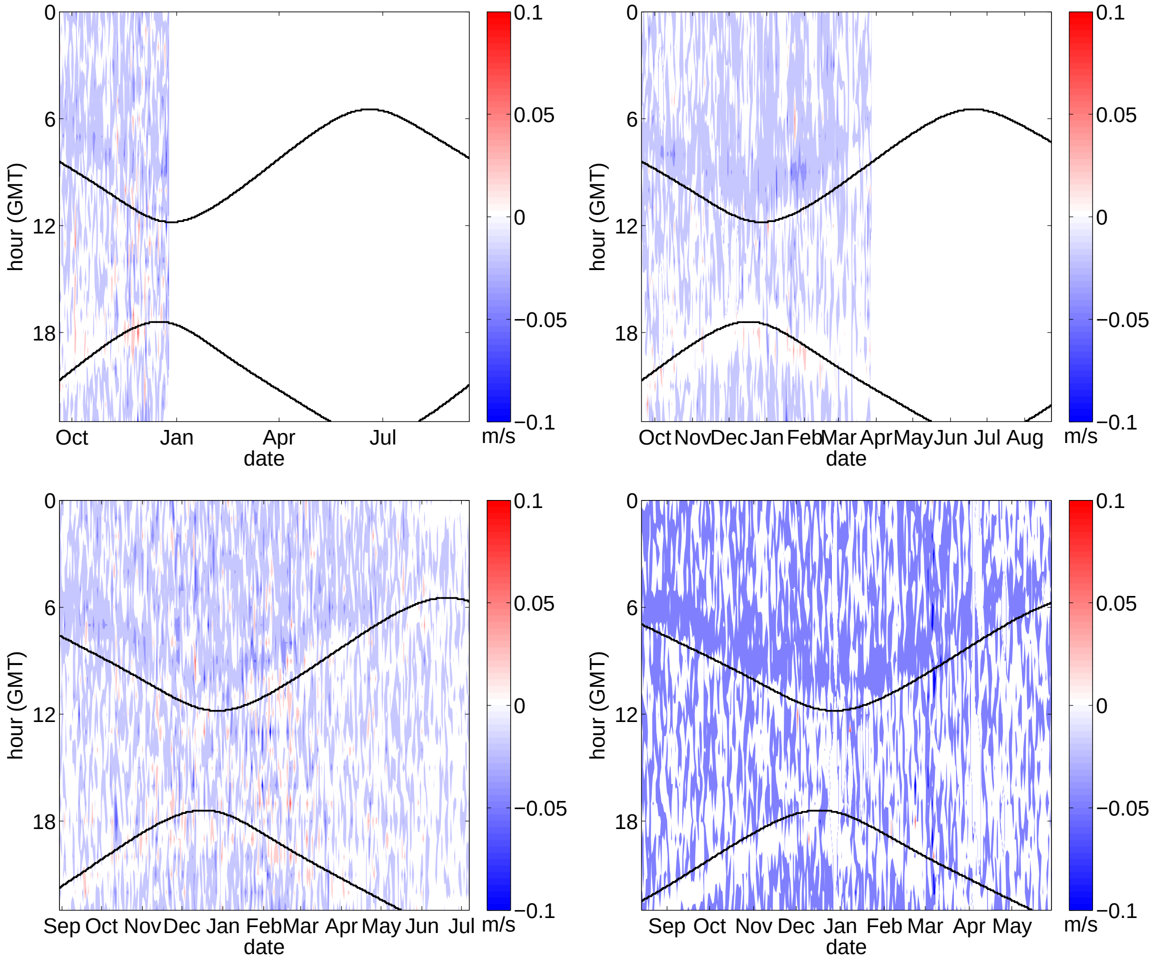

Figure 3: Mean vertical velocity anomaly in the upper 150m, broad black lines show time of sunrise and sunset. From left to right and top to bottom: cis04 (summer 2004 to summer 2005), cis05 (summer 2005 to summer 2006), cis06 (summer 2006 to summer 2007), cis11 (summer 2011 to summer 2012).

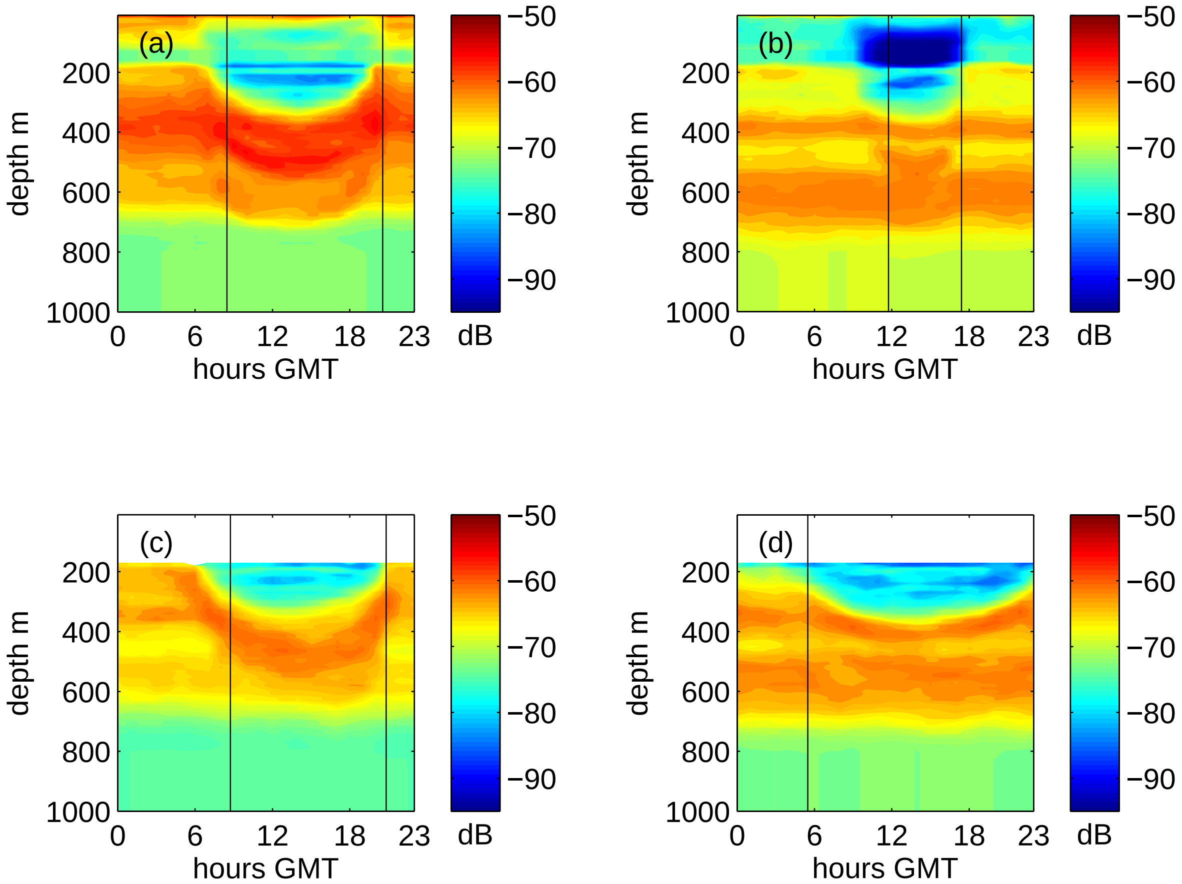

Figure 4: 7 day mean of targetstrength for: a) fall equinox, b) winter solstice, c) spring equinox, d) summer solstice during the cis04 deployment (summer 2004 to summer 2005). Black lines show time of sunrise and sunset. The left line corresponds to time of sunrise the right line to sunset. In cases where there is only one line visible this is sunrise, sunset is after 23 hours GMT.

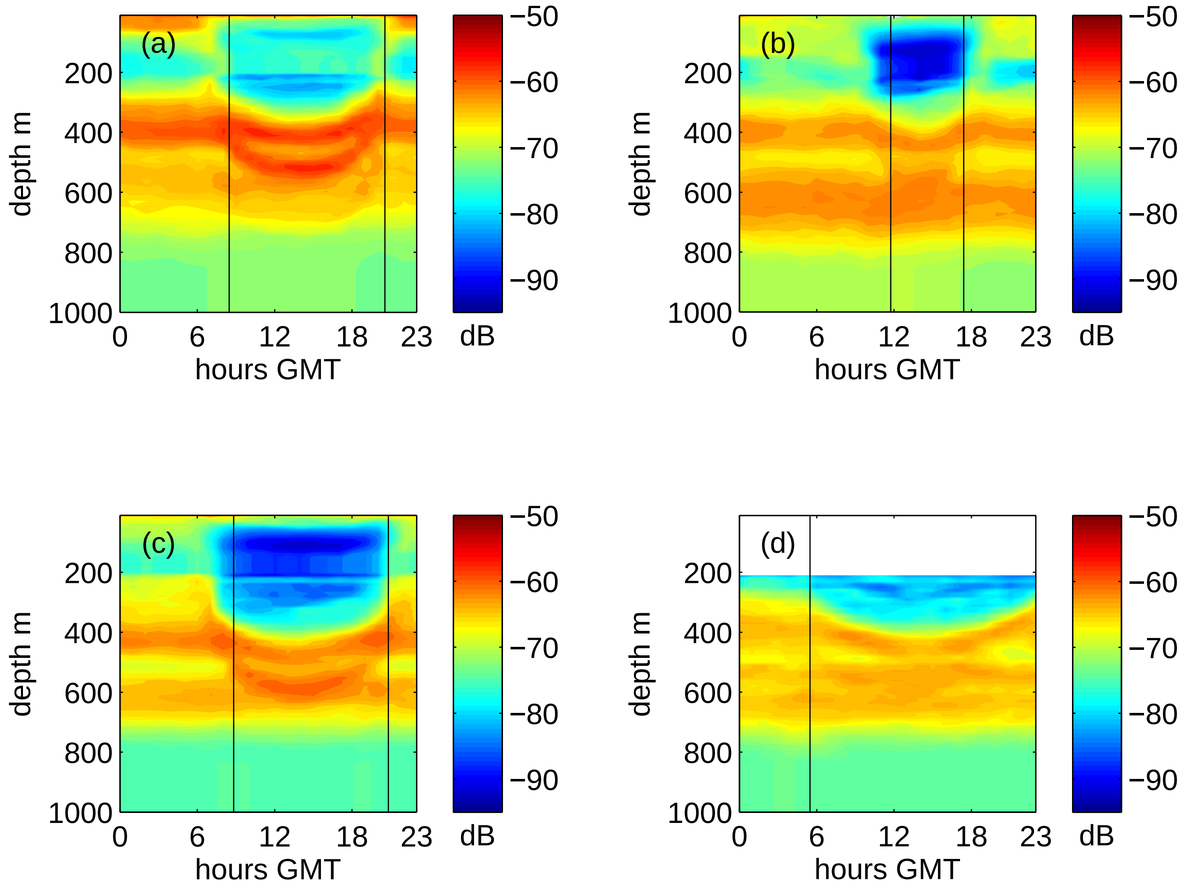

Figure 5: 7 day mean of targetstrength for: a) fall equinox, b) winter solstice, c) spring equinox, d) summer solstice during the cis05 deployment (summer 2005 to summer 2006). Black lines show time of sunrise and sunset. The left line corresponds to time of sunrise the right line to sunset. In cases where there is only one line visible this is sunrise, sunset is after 23 hours GMT.

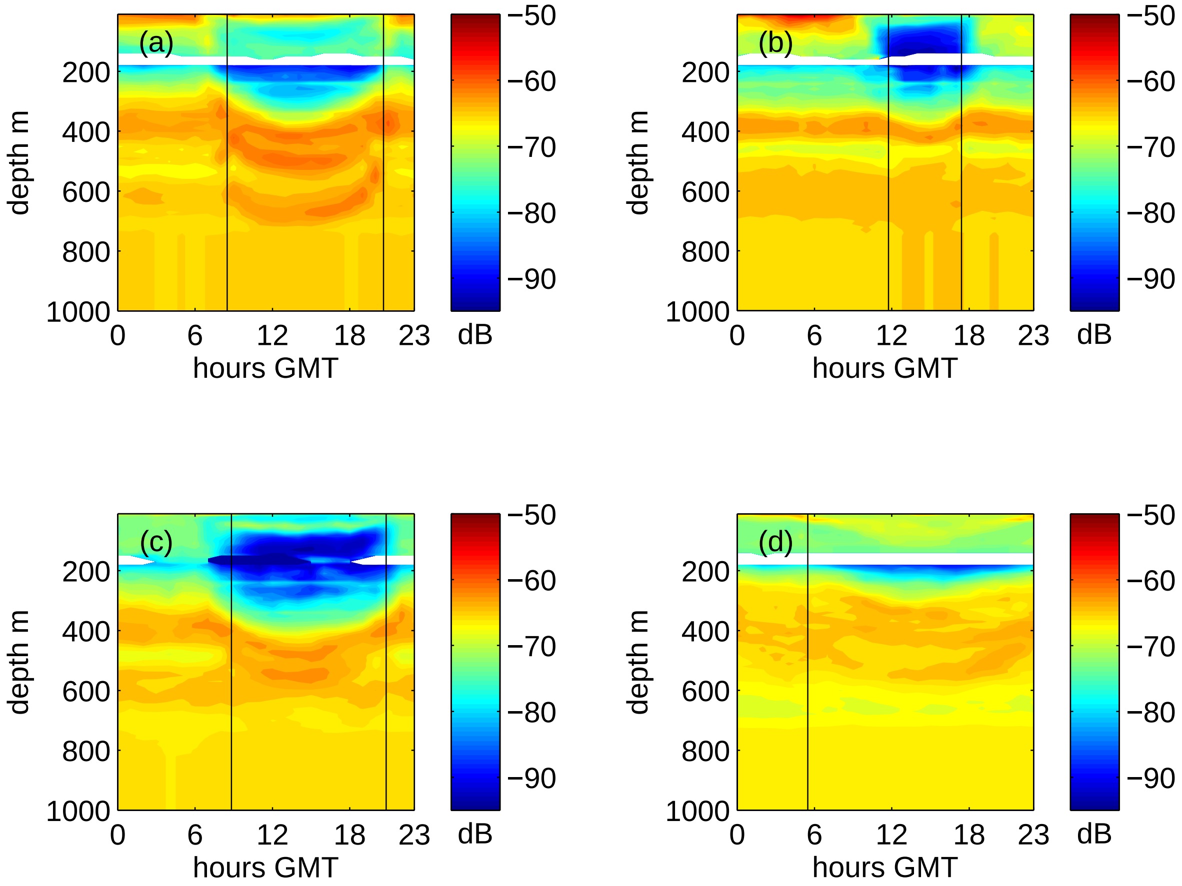

Figure 6: 7 day mean of targetstrength for: a) fall equinox, b) winter solstice, c) spring equinox, d) summer solstice during the cis06 deployment (summer 2006 to summer 2007). Black lines show time of sunrise and sunset. The left line corresponds to time of sunrise the right line to sunset. In cases where there is only one line visible this is sunrise, sunset is after 23 hours GMT.

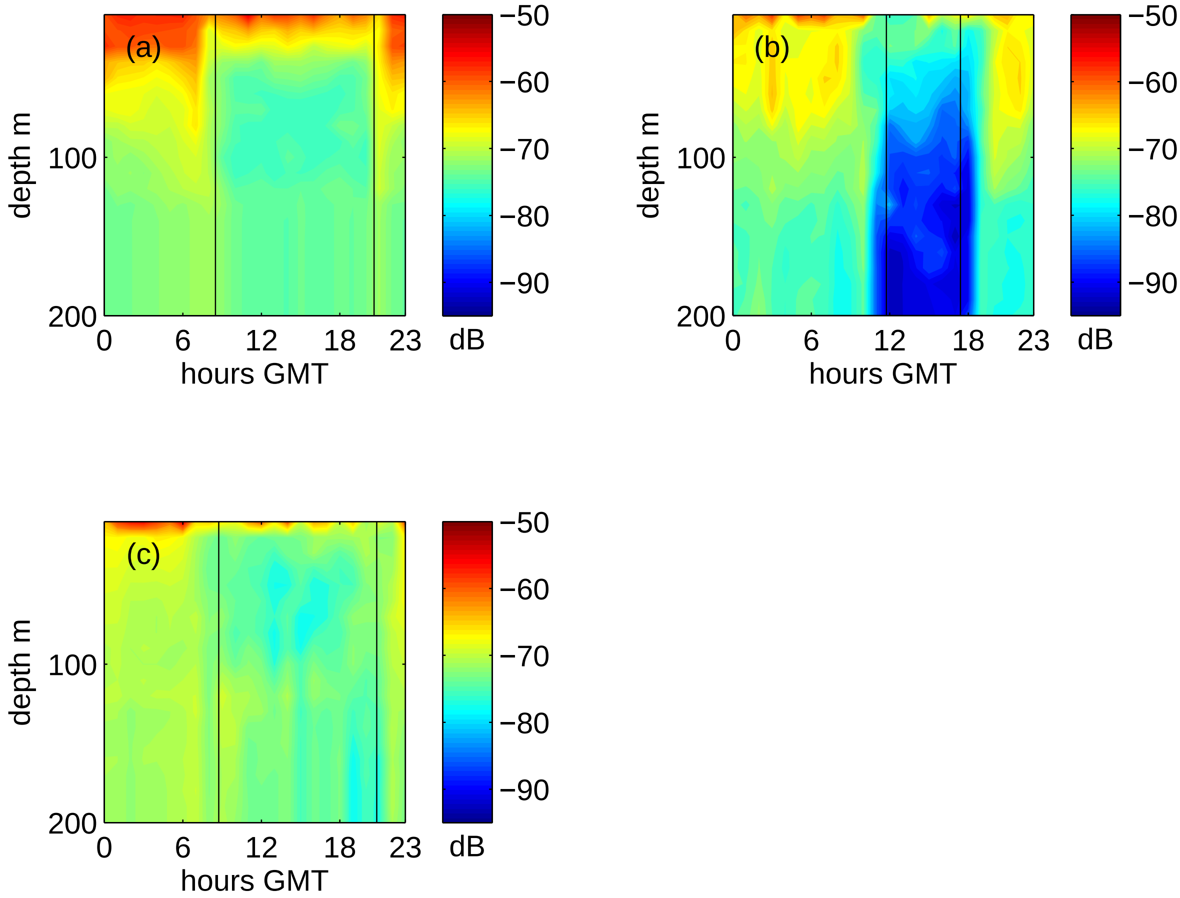

Figure 7: 7 day mean of targetstrength for: a) fall equinox, b) winter solstice, c) spring equinox, d) summer solstice during the cis11 deployment (summer 2011 to summer 2012). Black lines show time of sunrise and sunset. The left line corresponds to time of sunrise the right line to sunset. In cases where there is only one line visible this is sunrise, sunset is after 23 hours GMT.

not migrate below the depth of the scattering maximum at 600m that existed all day. The migration did not lead to a simple displacement of scattering layers downward but to a higher density of scatterers in the layers. During winter solstice (panels b)) there was hardly any displacement of the 400m layer, even during daytime and the 600m layer was not affected at all. During the time of the summer solstice (panels d)) no distinct layers were visible, the scatterers seem to be evenly distributed throughout the water column. Evacuation of the upper layers started one to two hours before sunrise, in the evening the targetstrength increases immediately after sunset. Throughout the solar year the shape of the daytime scatterer depleted upper layers changed but not the depth of the water column the scatterers evacuate. The steepness of the flanks of the evacuated zone stayed the same as well, leading to assume a faster continued descent/ascent to/from the noontime depth of the migrators after/before the initial descent/ascent in winter than in summer.

3.3 Seasonal Cycles

3.3.1 Vertical structure in relation to mixed layer depth

All three deployments that had a downward looking ADCP showed three distinct scattering layers. The uppermost, between 150m and the sea surface, existed only from April to December and followed the mixed layer depth (Figure 8 to 11). The two deeper layers were found between 250m and 500m and 500m and 750m, respectively. Both layers showed a synchronous seasonal cycle with maxima in June/July and October/November and minima in March and August/September. This second one, however, was not as pronounced as the March minimum.

The scattering layer in the upper 150m was only present and following the mixed layer during nighttime (middle and bottom panels of figures 8 to 11). Targetstrength maxima at the sea surface were most probably caused by the strong echo of the surface itself and bubbles entrained into the upper few meters due to turbulence and not by the presence of zooplankton as scatterers.

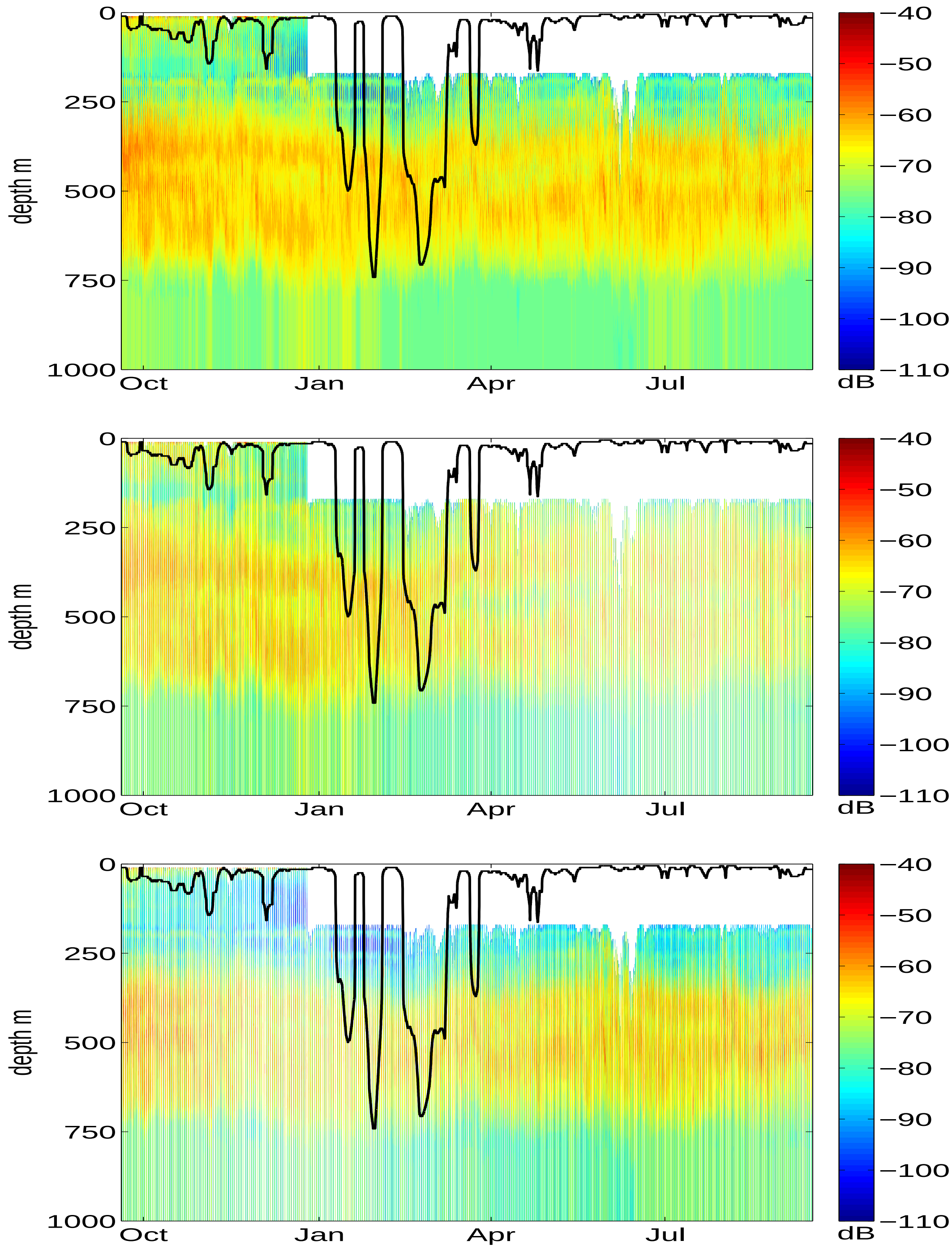

Figure 8: Targetstrength during the cis04 deployment (summer 2004 to summer2005), middle panel during night, lower panel during day. Black line shows depth of mixed layer.

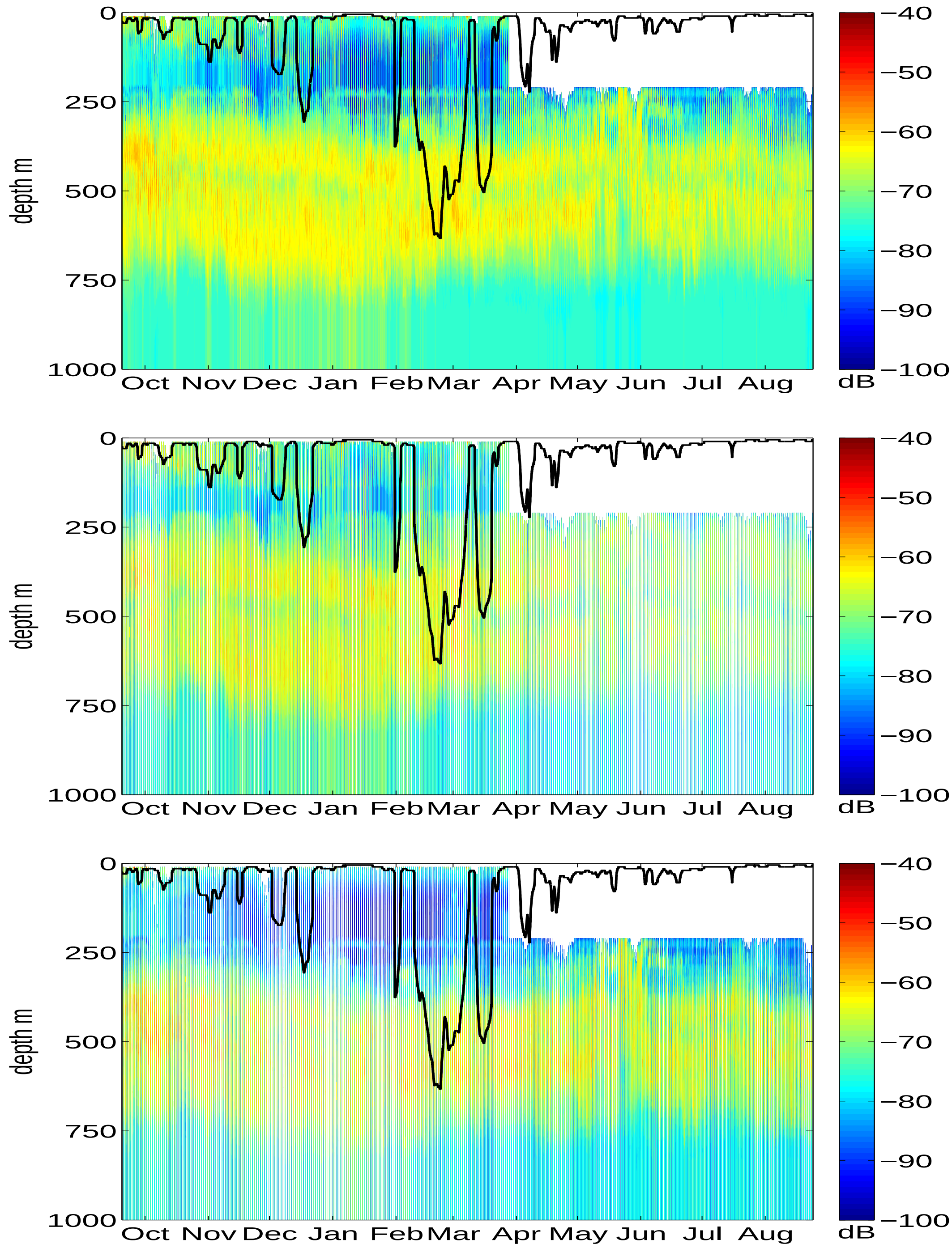

Figure 9: Targetstrength during the cis05 deployment (summer 2005 to summer2006), middle panel during night, lower panel during day. Black line shows depth of mixed layer.

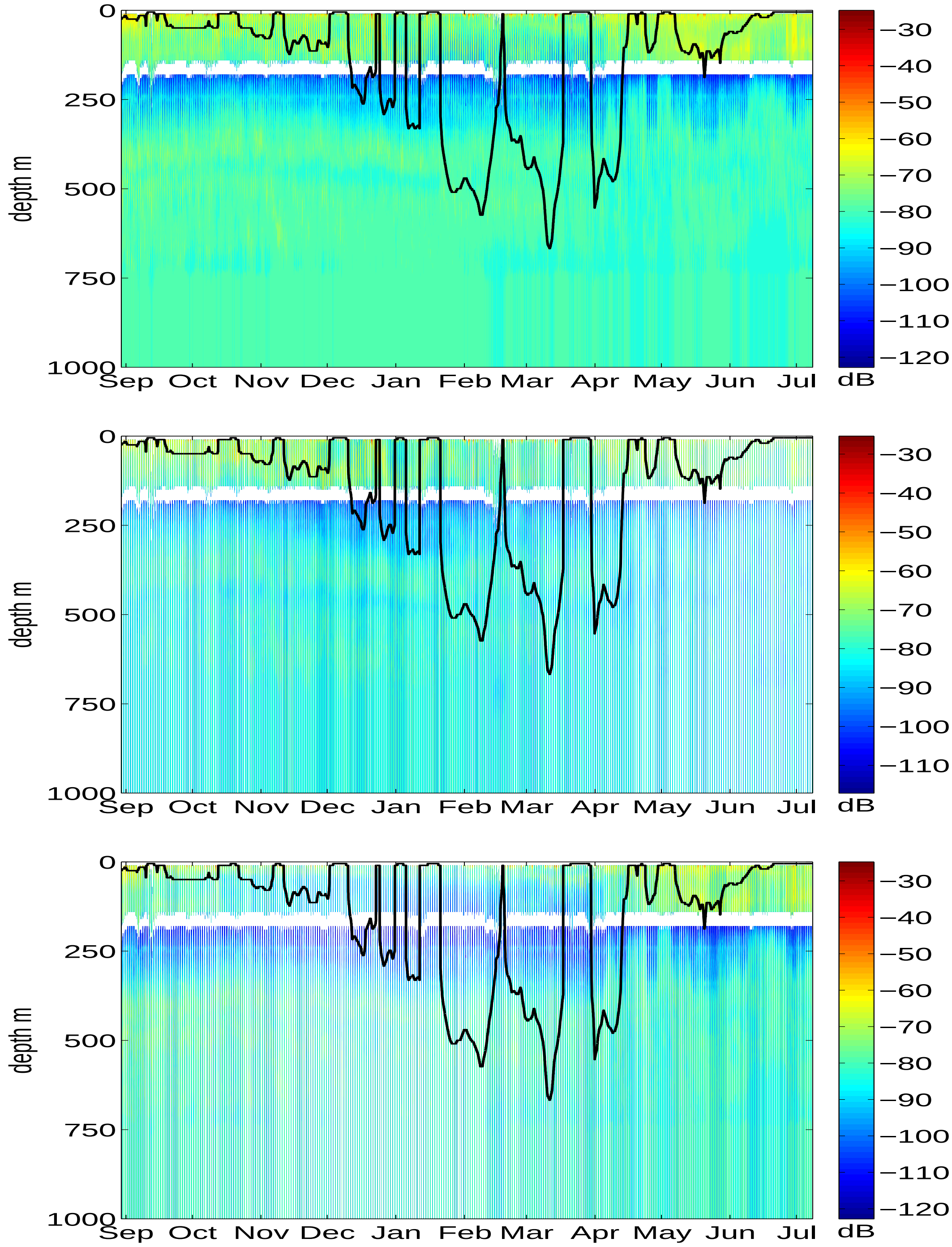

Figure 10: Targetstrength during the cis06 deployment (summer 2006 to summer 2007), middle panel during night, lower panel during day. Black line shows depth of mixed layer.

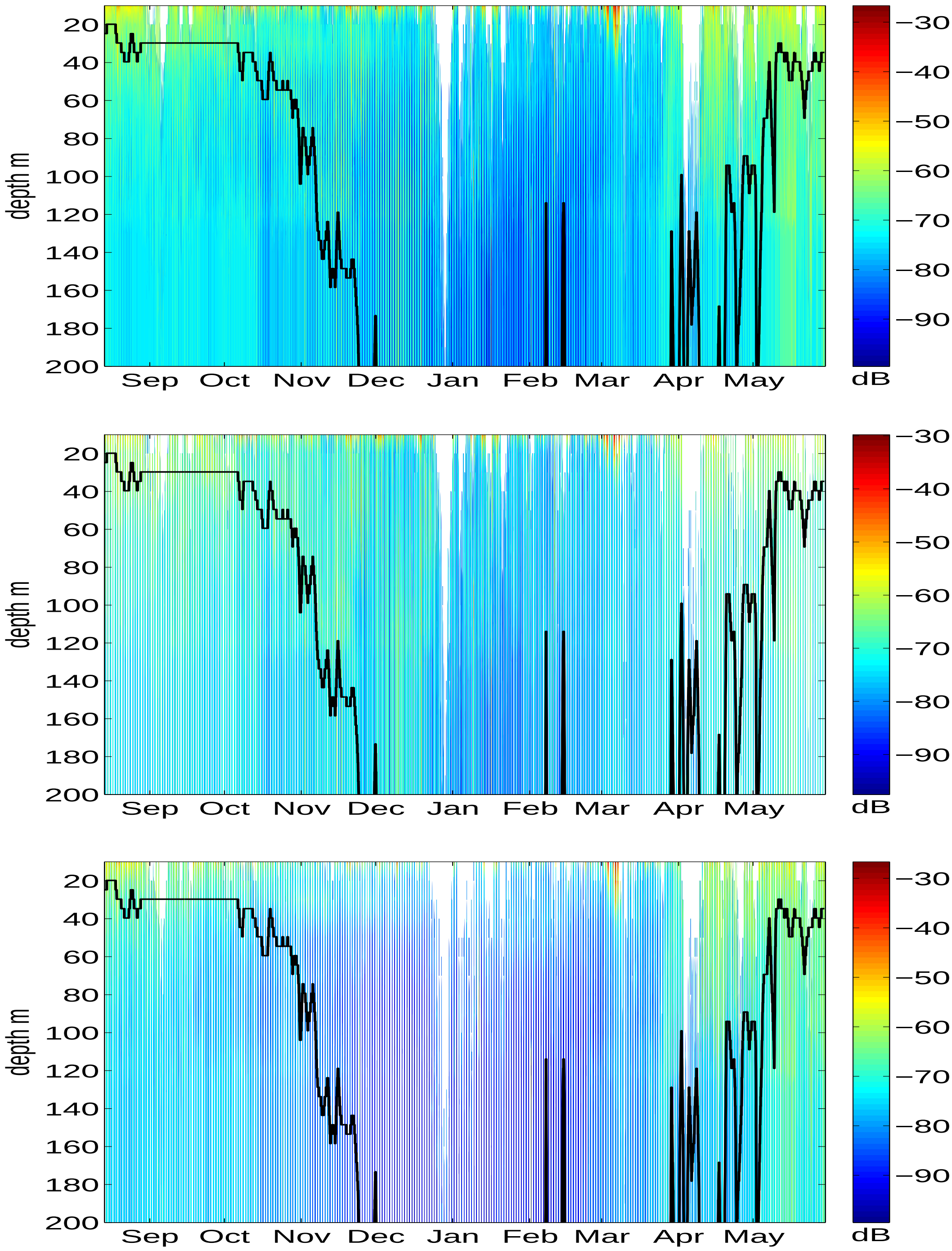

Figure 11: Targetstrength during the cis11 deployment (summer 2011 to summer 2012), middle panel during night, lower panel during day. Black line shows depth of mixed layer.

Table 4: Correlation coefficient rho between daily mean target strength (overall, nighttime and daytime) and mixed layer depth for cis$*$ from 0 to 200m, 200 to 400m and 400 to 600m. The parameter rho thereby denotes Pearson's linear correlation coefficient. Values in brackets are not significant when testing against zero correlation hypothesis.

Name	rho_0-200m	rho_200-400m	rho_400-600m
cis04	–	0.2368	(0.0084)
cis04_day	–	0.3721	(0.1024)
cis04_night	–	–	-0.1251
cis05	–	(0.0744)	-0.4251
cis05_day	–	0.2397	-0.3416
cis05_night	–	(0.0352)	-0.4351
cis06	0.5244	0.2740	-0.1131
cis06_day	0.4693	0.3780	(-0.1052)
cis06_night	0.4140	0.1662	-0.1481
cis11	0.6461	–	–
cis11_day	0.5249	–	–
cis11_night	0.6681	–	–

Mean daily targetstrength and mixed layer depth were tested for significant correlations in different depth bins (table 4). A high positive value means that there is stronger backscatter when there is a shallower mixed layer and weaker backscatter when there is a deeper mixed layer and vice versa for negative values. Correlation between 200 and 400m depth was positive and higher during daytime than during nighttime. With the exception of cis04 and cis04_day, the correlation in the 400-600m bin was negative, also the positive values were not significant. During cis04 and cis06, the correlations were weak and partly not significant but during cis05 they were strongly negative with values lower than -0.34, more measurements from this depth are necessary to be able to decide what the predominant behaviour is.

4 Discussion

For the evaluation of vertical velocity I assumed, that since vertical velocities in the ocean are generally low, the signal I see in the ADCP vertical velocity data is caused by the vertical migration of scatterers and not by vertical advection of the scatterers. The temporal pattern of the vertical velocities seen in figure 3 is consistent with the findings of *Heywood* (1996) in her study of diel vertical migration of zooplankton in the Northeast Atlantic. She suggests that the descent one hour before dawn may be due to some species having an internal clock which is set to mirror the suncycle. The author also raises the question if some zooplankton species may be able to detect UV radiation which would precede dawn in the visible spectrum by more than half an hour. The mean ascent and descent velocities tally with measurements from previous studies. *Cisewski et al.* (2010) measured monthly mean of daily maximum vertical velocities of $-1.5\ cm/s$ for the descent and $1.6\ cm/s$ for the ascent in their 2005 study of vertical migration in the Lazarev Sea, Antarctica. Values of a similar range were observed by *Heywood* (1996) for shallow migrators whose depth range is similar to the range of the upward looking ADCPs. Measurements of deep migrators from the same study show vertical velocities of $2-4\ cm/s$ in some cases even in excess of $4\ cm/s$ a value also measured by *Jiang* *et al.* (2007) who recorded maximum values of over 5 cm/s. Vertical advection through tides may bias the measurement of migration speeds. To gain more accurate velocity measurements the effect of tides on vertical migration at the CIS site would need to be examined.

As soon as stratification set in in April during the cis06 deployment the zooplankton appear to cease migration. This behavior continues until September. The same pattern could be seen during the cis11 deployment, unfortunately the upward looking ADCP failed during the cis04 and cis05 deployments so that we do not know whether the cessation of migration takes place during those years (Figure 2). The observed pattern might be explained by a stop of DVM in favour of feeding at the surface during a phytoplankton bloom. However, targetstrength in the whole water column still showed a diel cycle for this period, leading to different conclusions. One is, that during summer the concentration of backscatterers in the upper 150m is higher than in winter due to increased phytoplankton and non-migrating zooplankton concentrations weakening the diel migration signal, the other, that only part of the zooplankton continue migration whilst the remainder stays in the surface layer to feed.

This behaviour is also seen in some of the the data collected by *Cisewski et al.* (2010) and *Fortier et al.* (2001) though with some differences in expression. Another cause of the increased backscatter in the upper 150m during summer might be that a larger fraction of zooplankton migrates towards the surface. This is supported by the decreased backscatter at the resting depths of 400 and 600m. Seasonally migrating copepods (for example *Calanus finmarchicus, Pareuchaeta norvegica, Oithona* spp. which all spend the winter below 200m and congregate in the upper 200m in spring and early summer) increasing the backscatter in the upper 200-100m regardless of daytime might also contribute to the observed pattern (*Gislason*, 2003). Other species might also play a role as scatterers such as euphasids and crustaceans.

As the scatterers following the mixed layer depth can only be seen in the nighttime data and only during the time of the summer mixed layer shoaling, I conclude that the zooplankton ascend no higher than the bottom edge of the mixed layer to feed on organic detritus and graze on phytoplankton accumulated there. Phytoplankton accumulate at the bottom of the mixed layer to profit from nutrients entrained into the mixed layer from the more nutrient rich deep possibly forming a deep chlorophyll maximum on which the zooplankton can graze. The density jump at the bottom of the mixed layer can lead to the accumulation of detritus on top of this surface. During winter, when the mixed layer includes virtually the whole water column, zooplankton continue to migrate up to shallower regions during nighttime (Figure 2) but distribute more evenly so that no distinct scattering layer is visible in the upper 200m. This more even distribution mirrors the distribution of their food source which is mixed over the whole depth of the mixed layer by convection. The zooplankton do however continue to migrate downwards to their resting depths at 400 and 600m. The March minimum in the depth of the deep scattering layers may be explained by the zooplankton moving their daytime resting depth below the mixed layer to escape the strong convection therein. It is interesting to note that the seasonal cycle of the position of the deep scattering layer is opposite to that observed in the Greenland Sea where the deep scattering layer is found at 200m depth in winter and 400m depth in autumn and spring (*Fischer and Visbeck*, 1993).The deep resting depths seem to be inhabited during nighttime as well as during daytime suggesting that only a fraction of the plankters migrate upwards to feed. This is also true for some seasonally migrating species, for example only a small part of the copepod *Oncaea* spp. migrates upwards during spring and summer with the bulk remaining between 400 and 1600m depth (*Gislason*, 2003). Backscatter in the deep layers may also be caused by fish which in part also exhibit diel vertical migration and/ or seasonal migration (*Magnússon*, 1996). The existence of two resting depths and their existence regardless of time of day from fall to spring points to the participation of more than one species and developmental stage of zooplankton. The plankters which remain at depth during nighttime might be such individuals which have built up lipid reserves and therefore do not have the need to migrate upwards in order to feed and can therefor remain in the comparatively safer deep (*Hays*, 2003). During the summer the deep scattering layers are no longer as clearly defined as in winter, suggesting that

fewer plankters remain at depth even during the day in favour of feeding in the now food richer surface layers. *Fortier et al.* (2001) found that lager herbivore copepod species ascended to the surface layer for a shorter length of time and smaller omnivores stay in shallower water throughout the time of the midnight sun which may also lead to the blurring of layers during summer. In his 1995 study of seasonal migration of calanoid copepods in the Greenland Sea *Richter* (1995) found, that seasonally migrating species were predominantly herbivorous and non-migrating species were omnivorous. If a study at the CIS site were to be made using net tows or videosystems it would be interesting to sea weather this also holds true for the seasonal migrators in the Central Irminger Sea. A study of the species involved might also make it possible to find out if invertebrate predation has an effect on the seasonal migration (*Richter*, 1995).
The fact that the correlation between targetstrength and mixed layer depth in the upper 200m is high and the values are similar regardless if it is day or night might simply show that in summer, when the mixed layer is generally shallow, the amount of scatterers in the surface layer regardless of daytime is higher than in winter when zooplankton concentrations are lower. The same effect may come into play when explaining the high correlation coefficient in the 200-400m depth bin during daytime. Because mixed layer depth is not independent of season the correlation coefficient may show effects of, for instance, number of daylight hours and/or phytoplankton concentration.

5 Conclusion and Summary

The results presented above all indicate the existence of normal DVM at the CIS site with a daytime resting depth of more than 400m. The signal of the seasonally migrating copepods (*Gislason*, 2003) in the area might also have been picked up. Vertical velocities during the ascent were measured to be between 1 and 2 cm/s and between 2 and 4 cm/s during the descent.This value is within the range of vertical velocities measured by other authors: 2 to 6 cm/s (*Heywood*, 1996), up to 1.6 cm/s (*Cisewski et al.*, 2010) and up to 5.4 cm/s (*Jiang et al.*, 2007). The multiple scattering layers seen in the targetstrength data point to the participation of more than one species and developmental stage of zooplankton. The depths of the deep scattering layers correspond to the depths measured by *Magnússon* (1996) in the Irminger Sea. The mixed layer depth seems to influence the DVM but more detailed studies as to the exact causes of changes in DVM need to be made. It would be necessary to distinguish clearly between the influence of the mixed layer depth itself and the influence of phenomenons linked to mixed layer depth or the causes of different mixed layer depths on DVM. To understand the effects of DVM at the CIS site on higher trophic levels or carbon and nutrient cycling it is important to study which species and developmental stages perform DVM or seasonal migration and to what extent. This may be achieved through the deployment of camera systems at the CIS site and/or a series of net tows in different depths and seasons. Long term measurements of this kind may be able to reveal correlations between DVM and changes in population of planktivorous fish or invertebrates as suggested by *Hays* (1995).

References

Benoit-Bird, K. J., The effects of scattering-layer composition, animal size, and numerical density on the frequency response of volume backscatter, *ICES Journal of Marine Science: Journal du Conseil*, *66*(3), 582–593, 2009.

Benoit-Bird, K. J., W. W. L. Au, and D. W. Wisdom, Nocturnal light and lunar cycle effects on diel migration of micronekton, *Limnology and Oceanography*, *54*(5), 1789–1800, doi:10.4319/lo.2009.54.5.1789, 2009.

Cisewski, B., V. Strass, M. Rhein, and S. Krägefsky, Seasonal variation of diel vertical migration of zooplankton from ADCP backscatter time series data in the Lazarev Sea, Antarctica, *Deep Sea Research I*, *57*, 78–94, doi:10.1016/j.dsr.2009.10.005, 2010.

de Boyer Montégut, C., G. Madec, A. S. Fischer, A. Lazar, and D. Iudicone, Mixed layer depth over the global ocean: An examination of profile data and a profile-based climatology, *Journal of Geophysical Research: Oceans*, *109*(C12), n/a–n/a, doi:10.1029/2004JC002378, 2004.

Deines, K., Backscatter estimation using Broadband acoustic Doppler current profilers, in *Current Measurement, 1999. Proceedings of the IEEE Sixth Working Conference on*, pp. 249–253, doi:10.1109/CCM.1999.755249, 1999.

Fan, X., U. Send, P. Testor, J. Karstensen, and P. Lherminier, Observations of Irminger Sea Anticyclonic Eddies., *Journal of Physical Oceanography*, *43*(4), 2013.

Fischer, J., and M. Visbeck, Seasonal variation of the daily zooplankton migration in the Greenland sea , *Deep Sea Research Part I: Oceanographic Research Papers*, *40*(8), 1547 – 1557, doi:http://dx.doi.org/10.1016/0967-0637(93)90015-U, 1993.

Flagg, C. N., and S. L. Smith, On the use of the acoustic Doppler current profiler to measure zooplankton abundance, *Deep Sea Research Part A. Oceanographic Research Papers*, *36*(3), 455–474, 1989.

Fortier, M., L. Fortier, H. Hattori, H. Saito, and L. Legendre, Visual predators and the diel vertical migration of copepods under Arctic sea ice during the midnight sun, *Journal of Plankton Research*, *23*(11), 1263–1278, doi:10.1093/plankt/23.11.1263, 2001.

Gislason, A., Life-cycle strategies and seasonal migrations of oceanic copepods in the Irminger Sea, *Hydrobiologia*, *503*(1-3), 195–209, doi: 10.1023/B:HYDR.0000008498.87941.7d, 2003.

Hays, G., A review of the adaptive significance and ecosystem consequences of zooplankton diel vertical migrations, *Hydrobiologia*, *503*(1-3), 163–170, doi: 10.1023/B:HYDR.0000008476.23617.b0, 2003.

Hays, G., C. Proctor, A. John, and A. Warner, Interspecific differences in the diel vertical migration of marine copepods: the implications of size, color, and morphology, *Limnology and Oceanography*, *39*(7), 1621–1629, 1994.

Hays, G. C., Zooplankton avoidance activity, *Nature*, *376*(6542), 650–650, 1995.

Heywood, K. J., Diel vertical migration of zooplankton in the Northeast Atlantic, *Journal of Plankton Research*, *18*(2), 163–184, doi:10.1093/plankt/18.2.163, 1996.

Jiang, S., T. D. Dickey, D. K. Steinberg, and L. P. Madin, Temporal variability of zooplankton biomass from {ADCP} backscatter time series data at the Bermuda Testbed Mooring site , *Deep Sea Research Part I: Oceanographic Research Papers*, *54*(4), 608 – 636, doi:http://dx.doi.org/10.1016/j.dsr.2006.12.011, 2007.

Karstensen, J., ANIMATE Atlantic Network of Interdisciplinary Moorings and Time series for Europe: Calibration of Physical Data MicroCAT, TD-Logger, ADCP, RCM, 2005.

Lampert, W., The adaptive significance of diel vertical migrations, *Functional Ecology*, *3*, 21 – 27, doi:10.2307/2389671, 1989.

Longhurst, A., A. Bedo, W. Harrison, E. Head, E. Horne, B. Irwin, and C. Morales, NFLUX: a test of vertical nitrogen flux by diel migrant biota , *Deep Sea*

Research Part A. Oceanographic Research Papers, *36*(11), 1705 – 1719, doi: http://dx.doi.org/10.1016/0198-0149(89)90067-8, 1989.

Longhurst, A., A. Bedo, W. Harrison, E. Head, and D. Sameoto, Vertical flux of respiratory carbon by oceanic diel migrant biota , *Deep Sea Research Part A. Oceanographic Research Papers*, *37*(4), 685 – 694, doi:http://dx.doi.org/10.1016/0198-0149(90)90098-G, 1990.

Longhurst, A. R., and W. G. Harrison, Vertical nitrogen flux from the oceanic photic zone by diel migrant zooplankton and nekton , *Deep Sea Research Part A. Oceanographic Research Papers*, *35*(6), 881 – 889, doi:http://dx.doi.org/10.1016/0198-0149(88)90065-9, 1988.

Magnússon, J., The deep scattering layers in the Irminger Sea, *Journal of Fish Biology*, *49*, 182–191, doi:10.1111/j.1095-8649.1996.tb06075.x, 1996.

RDInstruments, Principles of Operation A Practical Primer, *Available from RDInstruments. com*, 1996.

Richter, C., Seasonal changes in the vertical distribution of mesozooplankton in the Greenland Sea Gyre (75 N): distribution strategies of calanoid copepods, *ICES Journal of Marine Science: Journal du Conseil*, *52*(3-4), 533–539, 1995.

Våge, K., et al., The Irminger Gyre: Circulation, convection, and interannual variability , *Deep Sea Research Part I: Oceanographic Research Papers*, *58*(5), 590 – 614, doi: http://dx.doi.org/10.1016/j.dsr.2011.03.001, 2011.

Waniek, J. J., and N. P. Holliday, Large-scale physical controls on phytoplankton growth in the Irminger Sea, Part II: Model study of the physical and meteorological preconditioning , *Journal of Marine Systems*, *59*(3â€“4), 219 – 237, doi: http://dx.doi.org/10.1016/j.jmarsys.2005.10.005, 2006.

Declaration

I confirm that my bachelor thesis

Temporal Variability of Zooplankton from ADCP Backscatter Time Series Data at the Central Irminger Sea (CIS) Site

is the result of my own work. No other person's work has been used without acknowledgment in the main text of this thesis.
All sentences or passages quoted in this thesis from other people's work have been specifically acknowledged by clear cross-referencing to author, work and pages.
The submitted written version of this thesis corresponds to the electronic storage device (1005653.pdf).

Kiel, June 23, 2014 Maren Elisabeth Richter